Cancer Cell
Article

Frequent Amplification of a chr19q13.41 MicroRNA Polycistron in Aggressive Primitive Neuroectodermal Brain Tumors

Meihua Li,[1] Kyle F. Lee,[1] Yuntao Lu,[1,11] Ian Clarke,[2] David Shih,[1] Charles Eberhart,[6] V. Peter Collins,[7] Tim Van Meter,[8] Daniel Picard,[1] Limei Zhou,[1] Paul C. Boutros,[5,8] Piergiorgio Modena,[9] Muh-Lii Liang,[10] Steve W. Scherer,[4] Eric Bouffet,[1] James T. Rutka,[2] Scott L. Pomeroy,[12] Ching C. Lau,[13] Michael D. Taylor,[2] Amar Gajjar,[14] Peter B. Dirks,[2] Cynthia E. Hawkins,[3] and Annie Huang[1,*]
[1]Division of Hematology-Oncology
[2]Division of Neurosurgery
[3]Department of Pathology
[4]The Center for Applied Genomics
Hospital for Sick Children, Toronto, ON M5G 0A3, Canada
[5]Ontario Institute of Cancer Research, Toronto, ON M5G 1X8, Canada
[6]Division of Pathology, John Hopkins University School of Medicine, Baltimore, MD 21205, USA
[7]Division of Pathology, University of Cambridge, Cambridge CB2ITN, UK
[8]Department of Neurosurgery, Virginia Commonwealth University, Richmond, VA 23298-063, USA
[9]Istituto Nazionale per lo Studio e la Cura dei Tumori, Milano, 210133, Italy
[10]Department of Neurosurgery, Taiwan Veteran's General Hospital, Taipei, Taiwan 11217, ROC
[11]Department of Neurosurgery, Nanfang Hospital, Guangzhou, 510515, China
[12]Department of Neurology, Children's Hospital Boston, Boston, MA 02115, USA
[13]Texas Children's Cancer Center, Baylor College of Medicine, Houston, TX 77030, USA
[14]Neuro-oncology Division, St. Jude Children's Research Hospital, Memphis, TN 38105-3678, USA
*Correspondence: annie.huang@sickkids.ca
DOI 10.1016/j.ccr.2009.10.025

SUMMARY

We discovered a high-level amplicon involving the chr19q13.41 microRNA (miRNA) cluster (*C19MC*) in 11/45 (~25%) primary CNS-PNET, which results in striking overexpression of miR-517c and 520g. Constitutive expression of miR-517c or 520g promotes in vitro and in vivo oncogenicity, modulates cell survival, and robustly enhances growth of untransformed human neural stem cells (hNSCs) in part by upregulating WNT pathway signaling and restricting differentiation of hNSCs. Remarkably, the *C19MC* amplicon, which is very rare in other brain tumors (1/263), identifies an aggressive subgroup of CNS-PNET with distinct gene-expression profiles, characteristic histology, and dismal survival. Our data implicate miR-517c and 520g as oncogenes and promising biological markers for CNS-PNET and provide important insights into oncogenic properties of the *C19MC* locus.

INTRODUCTION

Brain tumors are the leading cause of childhood cancer-related morbidity and mortality. Primitive neuroectodermal tumors (PNET), which are the most frequent malignant pediatric brain tumors, include medulloblastoma, a cerebellar PNET, and CNS-PNET (also called supratentorial PNET or sPNET)—an aggressive cerebral tumor (McLendon et al., 2007). Comprehensive genetic studies of a substantial number of CNS-PNET have not yet been undertaken due to their relative rarity. Lack of

SIGNIFICANCE

Lack of insight into disease mechanisms impedes development of effective therapies for many human neoplasms, including childhood brain tumors such as CNS-PNET. Through global genomic studies, we discovered a frequent high-level amplicon of a polycistronic miRNA locus (*C19MC*), which defines aggressive CNS-PNET, and provide functional evidence that *C19MC* miRNAs act as oncogenes. Interestingly, although *C19MC* amplification remains to be reported in other cancers, expression of *C19MC* miRNAs has also been linked to unfavorable breast cancer phenotypes. Together with our discovery of recurrent *C19MC* gene amplification in a highly malignant brain tumor, these data highlight *C19MC* as an attractive candidate biomarker and therapeutic target for aggressive human cancers and support an emerging theme that miRNAs are important determinants of tumor biology.

insight into the molecular pathogenesis of CNS-PNET is a major obstacle toward development of disease-specific models and treatments for these frequently fatal tumors.

CNS-PNET, which represent 3%–7% of all pediatric brain tumors, are a heterogeneous group characterized by primitive neuroepithelial cells with variable neuronal, glial, or ependymal differentiation. Unlike rhabdoid tumors, which are defined by *INI1* gene alterations (Allen et al., 2006), CNS-PNET may pose significant diagnostic challenges due to lack of characteristic genetic or immunohistochemical markers (McLendon et al., 2007). In addition to CNS-PNET, several other PNET histologic variants may arise in the cerebral hemispheres: these include ependymoblastoma and medulloepithelioma, which have characteristic histologic features such as ependymal rosettes and primitive neural tube formation, and ENATR, a newly described entity with ependymoblastic differentiation (Gessi et al., 2009; McLendon et al., 2007). Whether CNS-PNET and PNET variants represent distinct molecular tumor subtypes remains debated (Burger, 2006; Judkins and Ellison, 2008).

CNS-PNET and medulloblastoma share very similar histology and are largely distinguished by tumor location. However, CNS-PNET are more aggressive tumors with significantly inferior outcomes (Fangusaro et al., 2008; Timmermann et al., 2006) than medulloblastoma (Packer et al., 2006). Cumulative data suggest CNS-PNETs and medulloblastoma have distinct genetic features and histogenesis. Notably, CNS-PNET lack expression of cerebellar granule cell-specific transcription factors (Pomeroy et al., 2002) and isochromosome 17q (i17q), which characterize medulloblastoma (Inda et al., 2005; McCabe et al., 2006; Pfister et al., 2007) and rarely arise in murine medulloblastoma models (Zindy et al., 2003).

Limited CGH studies indicate CNS-PNETs are genetically heterogeneous with frequent but diverse copy number aberrations (CNAs). Genes targeted by CNAs in CNS-PNET remain largely unknown; to date, amplification of *MYCN*, *PDGFB* and *PDGFRA*, and *CDKN2A/2B* deletions have been reported (Inda et al., 2005; McCabe et al., 2006; Pfister et al., 2007). However, the significance of these and other reported genetic alterations to the biology and clinical phenotypes of CNS-PNET is not known.

MicroRNAs (miRNAs) are short ~22 nucleotide noncoding RNA that function as important regulators of gene expression in various cell types. They are implicated in diverse biological processes, including self-renewal and pluripotentcy (Bar et al., 2008), and as etiologic genes in various human malignancies (Esquela-Kerscher and Slack, 2006). Patterns of miRNA expression have been shown to distinguish tumor types and to predict tumor biology (Lu et al., 2005). Direct genetic alterations of a few miRNAs have also been reported in human cancers: these include MiR15/16a in CLL (Calin et al., 2002), MIR-17-92 in B cell lymphoma (He et al., 2005), and LET-7 in lung cancer (Johnson et al., 2005). Although miRNAs have been implicated in malignant gliomas (Papagiannakopoulos et al., 2008), their role in malignant pediatric brain tumors remains largely unexplored.

In this study, we sought to comprehensively define genetic alterations in CNS-PNET by performing high-resolution DNA copy number and gene expression analysis on a substantial number of primary tumors.

RESULTS

Identification of a Frequent High-Level Amplicon at chr19q13.41 in CNS-PNET

We performed high-resolution copy number and gene-expression analyses on 39 and 33 primary tumors, respectively (Table S1 available online). Global DNA copy number determined using the 500K Affymetrix SNP arrays and dChip analysis (Lin et al., 2004) revealed frequent and multiple CNAs (10–28/tumor) in most tumors (Figure S1; Tables S2 and S3) and collectively confirm prior observations (Inda et al., 2005; McCabe et al., 2006; Pfister et al., 2007) that CNS-PNET are a genetically heterogeneous but distinct group of embryonal brain tumors.

Despite substantial genomic heterogeneity, we observed recurrent chr2 gains and focal chr19q13.41 amplification in a significant proportion (8/39) of CNS-PNET. Two tumors had nonoverlapping chr2p24.3 and chr2q33.3 amplicons encompassing *MYCN* and putative oncogenes, *CREB1* and *FZD5* (Figure 1A); however, gene-expression profiles did not correlate *MYCN*, *CREB1*, or *FZD5* expression with chr2 gains in tumors (data not shown). In contrast, the chr19q13.41 amplicon in all eight tumors mapped to a common ~1 Mb interval between the *DPRX* and *LILRP2* loci (Figure 1B). Notably, the chr19q13.41 amplicon was absent in matched lymphocyte DNA of an additional tumor PNET 54 (Figure 1C), indicating it was tumor specific and not a normal DNA copy number variant (Iafrate et al., 2004). We used FISH analyses to validate the genotyping data (Figure 1D), and to test for the chr19q13.41 amplicon in five additional tumors that were not included in genotyping analysis. Collectively, the amplicon was detected in ~25% (11/45) of tumors analyzed, a remarkably high frequency indicating an important CNS-PNET oncogene(s) maps to chr19q13.41.

MicroRNAs of the *C19MC* Locus Are the Targets of the chr19q13.41 Amplicon

Genotyping and qPCR analysis indicated the minimal chr19q13.41 amplicon in CNS-PNET spanned 34 protein-coding loci and 2 miRNA clusters (Figures 2A and 2B). We examined transcriptional profiles of 33 CNS-PNET by t tests to determine if any coding loci exhibited copy number-driven changes in expression (Figure 2C); qRT-PCR validation of select genes is shown in Figure S2A. Only one gene exhibited a modest 2-fold increase in expression (*CNOT-3*; $p = 0.02$), indicating miRNA clusters as likely targets of the chr19q13.41 amplicon. The chr19q13.41 amplicon spans a large, poorly characterized, primate-specific miRNA cluster, *C19MC* and the *MIR-371-373* locus, which map ~100 kb apart. Although miR371-373 has been implicated in germ cell tumors (Voorhoeve et al., 2006), little is known regarding the oncogenic potential of the *C19MC* locus that encodes 54 predicted miRNA (Bentwich et al., 2005).

To identify potential oncogenic miRNAs, we used a miRNA array to assay expression of the *C19MC* and *MIR371-373* clusters (Table S4) in chr19q13.41-amplified tumors. These analyses revealed robust expression of several *C19MC* miRNAs in tumors relative to fetal brain, but only modest expression of miR371-373 (Figure 2D). With exception of miR-512-3p and 520c-3p, miRNA levels were confirmed by gene-specific qRT-PCR (Figures S2B–S2D) and significantly correlated ($p < 0.0001$) with chr19q13.41 amplification (Figure 2E). We observed highest tumor-specific

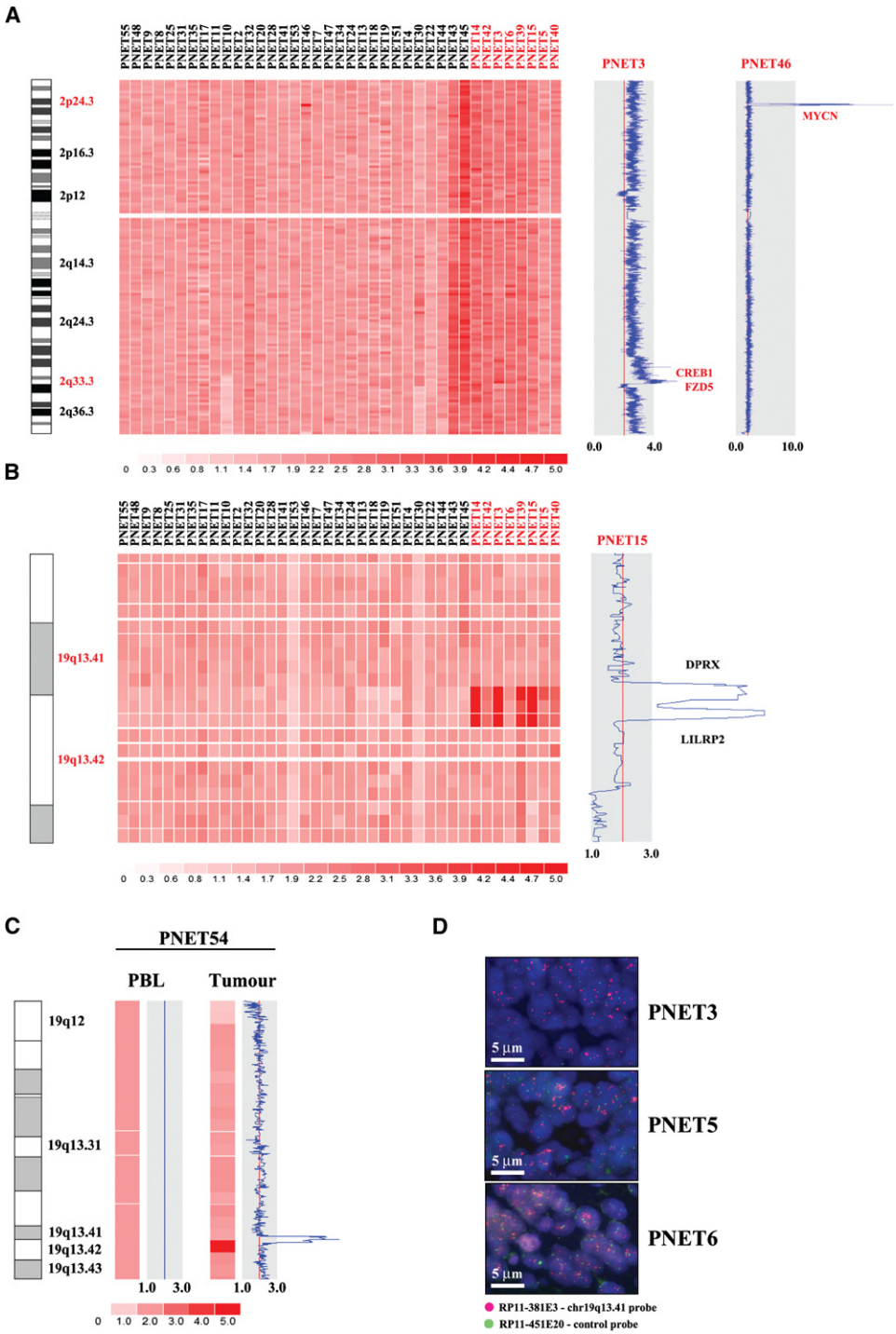

Figure 1. Frequent chr2 Gains and chr19q13.41 Amplication in CNS-PNET

Global DNA copy number profiles of 39 CNS-PNET were generated using the Affymetrix 500K SNP arrays (Figure S1). (A) and (B) show inferred DNA copy numbers as determined using dChip for SNPs on chromosomes 2 and 19 with DNA gains and losses indicated by shades of red.

(A) Expanded copy number profiles of chr2 showing frequent whole chr2 gains in tumors; amplicons encompassing *MYCN* and candidate oncogenes, *CREB1* and *FZD5*, in two individual tumors are shown on the right.

(B) Expanded view illustrating overlapping boundaries of the chr19q13.41 amplicon, which is flanked by the *DPRX* and *LILRP2* loci in 8/39 tumors (red labels). Copy number plot of an individual tumor is shown on the right.

(C) Inferred copy number plots generated using dChip pair-matched analysis reveals the chr19q13.41 amplicon in tumor, but not matched normal lymphocyte (PBL) DNA of PNET54.

(D) Fluorescence in situ hybridization confirms high-level chr19q13.41 DNA copy number gains and amplification, respectively, in tumors PNET 3 and 5 and 6 as indicated by genotyping analysis.

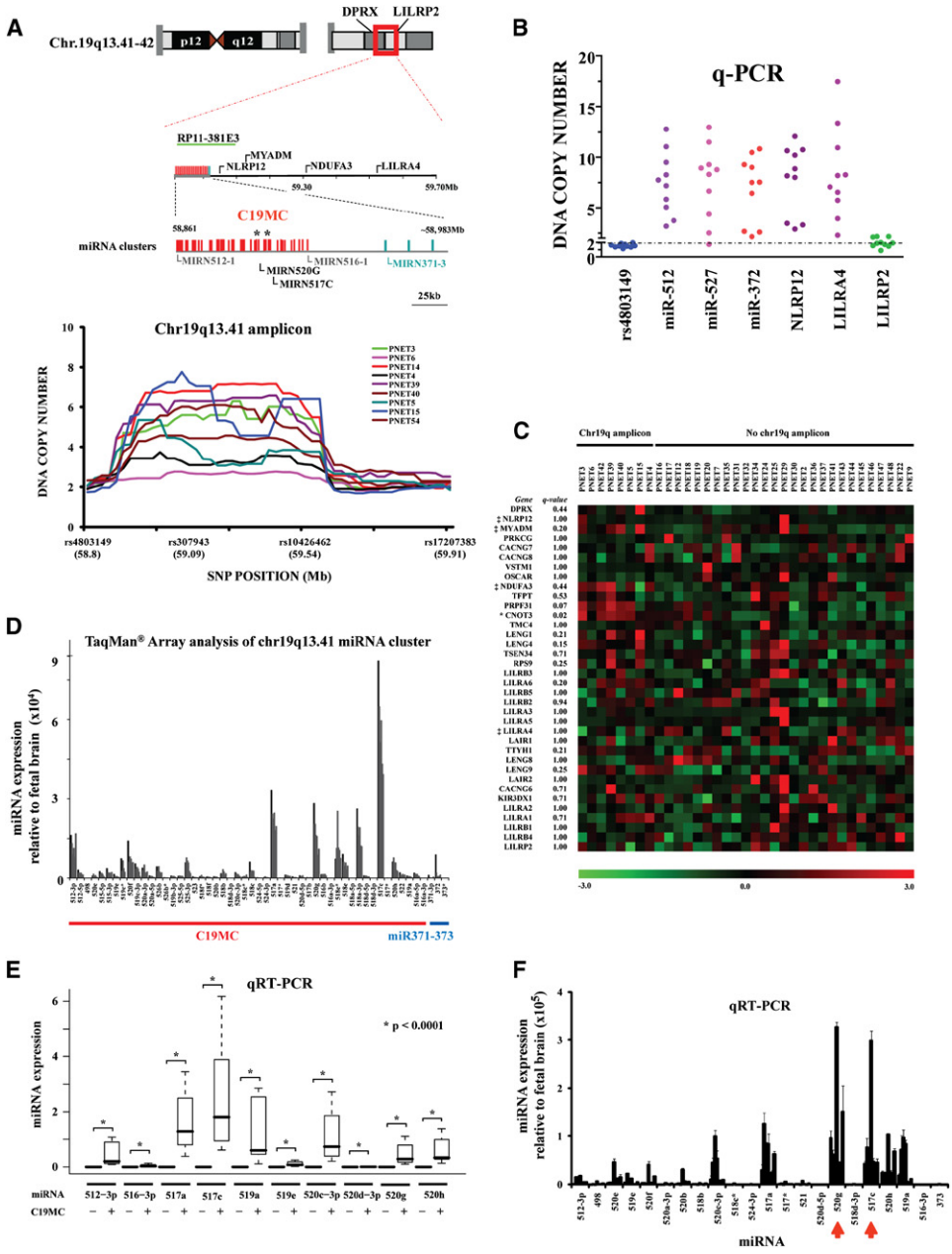

Figure 2. MicroRNAs Are the Oncogenic Target of the chr19q13.41 Amplicon

(A) Genomic organization of the chr19q13.41 amplicon, which maps between the *DPRX* and *LILRP2* loci, is schematized. Relative map positions of the chr19 microRNA cluster (*C19MC*) (red), the *MIR371-373* cluster (blue), and select coding genes within the amplicon boundaries are shown. Asterisks (*) mark candidate oncogenic *MIR-520g* and *517c*; *MIR-512-1* and *MIR-516-1*a mark the limits of the locus. BAC clone RP11-381E3, used for FISH analysis, is indicated in green. All map positions are based on the hg18 build from the UCSC Genome Database (http://genome.ucsc.edu/). Lower panel shows a DNA copy number plot of SNPs, indicating overlapping boundaries of the chr19q13.41 amplicon in nine tumors.

(B) Confirmation of chr19q13.41 amplicon boundaries in nine tumors by qPCR copy number analysis of select loci. Result is representative of two independent experiments.

(C) Heat map showing expression levels of 34 coding genes on chr19q13.41 as determined from BeadChiP expression analysis of 33 tumors; q values indicate significance of gene expression changes relative to chr19q13.41 amplification, asterisk (*) indicates the *CNOT3* locus which showed a modest 2-fold gene expression change in chr19q13.41 amplified tumors, and ‡ indicates select genes validated by qRT-PCR (Figure S2A).

(D) TaqMan microRNA array analysis of seven tumors with chr19q13.41 amplification indicate high expression of several *C19MC* miRNAs (miR-512-3p, 517a, 520g, 517c, 519a), but not miR371-373, in tumors relative to fetal brain (Figures S2B–S2D).

(E) Box and whisker summary plot showing expression levels of ten select *C19MC* miRNA relative to chr19q13.41 amplification in tumors; qRT-PCR analysis of eight amplified and 15 nonamplified tumors is shown. Paired boxes represent the 25th–75th percentile expression values for each miRNA in tumors without (–) and with (+) the *C19MC* amplicon. Horizontal bars indicate median, while vertical lines indicate maximum and minimum miRNA expression values for each tumor group; asterisks (*) denote significant correlation of miRNA expression levels with *C19MC* amplification; and error bars represent SEM of $n \geq 2$ with three replicas.

expression (up to 40× greater than other miRNAs) of miR-520g and miR-517c in chr19q13.41-amplified tumors (Figure 2F) and, therefore, focused on miR-520g and 517c to test for oncogenic potential of the *C19MC* locus.

miR-520g and 517c Have Oncogenic Effects In Vitro and In Vivo

To test if miR-520g and 517c have oncogenic properties, we characterized the effects of stable miRNA expression (Figure 3A) in hemispheric PNET (PFSK) and medulloblastoma (Daoy) cell lines, which have low endogenous miR-520g and 517c expression (Figure S3), as well as murine NIH 3T3 cells using growth, soft agar transformation and nude mouse xenograft assays. Although, the *C19MC* locus is primate specific, we hypothesized that genes with important oncogenic functions will target conserved, critical downstream pathways across species and cell types. Indeed, miR-520g or 517c expression enhanced cell growth and/or transformation in all three cell types (Figures 3B–3D). Interestingly, we observed cell-type and miRNA-dependent phenotypic changes that were not associated with relative miRNA levels. While miR-517c expression enhanced growth of all three lines ($p < 0.001$) and promoted soft agar growth and xenograft Daoy, NIH 3T3-miR-517c cells exhibited limited in vitro transformation (Figure 3C) but formed robust xenografts (Figure 3D). Similarly, miR-520g expression had limited effects on cell growth (Figure 3B) but promoted soft agar growth and xenograft formation in Daoy and NIH 3T3 cells (Figures 3C and 3D). These observations collectively support oncogenic functions for miR-520g and 517c and suggest that, like other oncogenic miRNAs (Bonci et al., 2008), miR-520g and 517c may effect cell transformation via multiple mechanisms.

miR-520g and 517c Expression Promotes Cell Survival and Inhibits Neural Stem Cell Differentiation

To investigate how miR-520g or 517c might drive oncogenesis, we examined tumor transcriptional profiles to identify gene-expression changes most significantly correlated with *C19MC* amplification using t test statistics (Figure 4A). A resulting set of 381 and 501 genes, respectively, with up- and downregulation (Table S5) in *C19MC*-amplified tumors were further investigated using the gene function annotation tool GOSTAT (Beissbarth and Speed, 2004) (Table S6). Interestingly, apoptosis regulators were significantly downregulated in *C19MC*-amplified tumors (22 of 501 genes, $p = 5.57E{-}8$); 11/22 genes, including *API5*, *BAD*, and *TRADD*, had proapoptotic functions. Consistent with these observations, miR-520g or 517c expressing PFSK, Daoy, and NIH 3T3 cells exhibited increased cell viability and decreased apoptosis in serum-deprived media (Figures 4B and 4C). Collectively, these data indicate that miR-520g and 517c promote oncogenesis in part by modulating cell survival pathways.

Interestingly, GOSTAT analyses also revealed enrichment of developmental signaling genes in *C19MC*-amplified tumors (83 of 381 genes, $p = 4.79E{-}26$; Table S6). In particular, self-renewal and survival genes, including *SOX11*, *NR2F1*, *NKX2-2*, *FGF13*, *FGFr3*, *SALL4*, and WNT pathway ligands (*WNT5A* and *-7A*) and receptors (*FZD2*, *-3*, *-7*, and *-10*) were overrepresented. We investigated if ectopic miR-520 g or 517c expression could alter the phenotype of primary human neural stem cell line (hNSC), which normally continually replicate in growth-promoting/proliferative media containing high FGF and EGF, but undergo growth arrest in factor-deprived/differentiation conditions such as 10% serum media (Sun et al., 2008). Stable hNSC-miR-520g and 517c cells did not exhibit significant changes in growth under proliferative conditions (Figure S4); however, miR-520g and to a lesser extent, miR-517c expression, strikingly enhanced hNSC growth in differentiation media (Figures 5A and 5B; Figure S4), indicating that miR-520g or 517c may alter the differentiation potential of hNSCs.

We used immunocytochemical and qRT-PCR analyses to compare expression of Tubulin β-III and GFAP, which respectively mark neuronal and astrocytic differentiation, in hNSC-miR-520g and 517c cells grown in proliferative and differentiation conditions. GFAP expression was not significantly altered in hNSCs-miR-520g and 517c cells as compared to controls (data not shown). Notably, although hNSCs-miR-520g or 517c cells did not exhibit significant changes in Tubulin β-III expression under proliferative conditions, Tubulin β-III expression in hNSC-miR-520g cells grown in differentiation media was strikingly diminished as compared to controls (15% versus 65% Tubulin β-III positivity; Figures 5C and 5D). Interestingly, qRT-PCR analysis revealed expression of *NKX2-2* and *OLIG1*, two genes with essential roles in normal neuronal cell-fate specification and differentiation (Briscoe et al., 2000; Zhou and Anderson, 2002), was also diminished in miR-520g, as well as 517c-expressing hNSCs (Figure 5D). We also observed that robust effects of miR-520g on hNSC differentiation was accompanied by striking changes in expression of neural stem/progenitor cell markers in hNSCs grown under differentiation conditions. Specifically, qRT-PCR analysis revealed upregulation of early neural stem/progenitor cell markers *CD44*, *CD133*, and *POU3F2* in stable hNSC-miR-520g, as well as 517c cells grown in proliferative media, but only hNSC-miR-520g cells maintained or exhibited robust expression (~3- to 7-fold greater than controls) of neural stem/progenitor cell markers in differentiation media (Figure 5E). These data suggest that miR-520g, and to a more limited extent, miR-517c, promotes hNSC growth by restricting differentiation and enhancing neural stem/progenitor cell phenotypes.

Interestingly, expression of several *C19MC* miRNAs, including miR-520 g, has also been correlated with human ES cell (hESC) differentiation (Bar et al., 2008). Together with our observations, these data highlight an important role for miR-520g and possibly other oncogenic *C19MC* miRNAs in maintenance of primitive/progenitor cell phenotypes.

miR-520g Expression Correlates with Altered WNT Signaling

Substantial data implicate aberrant developmental signaling in the pathogenesis of embryonal brain tumors, including

(F) Gene-specific qRT-PCR confirms high expression of select *C19MC* miRNAs in chr19q13.41-amplified tumors relative to normal fetal brain (Figure S2); miR-520g and 517c had highest tumor-specific expression (red arrows) in seven tumors analyzed; error bars represent SD of $n \geq 2$ experiments (3 replicas/experiment); and miRNA levels shown in (D–F) were determined relative to *RNU6B* control.

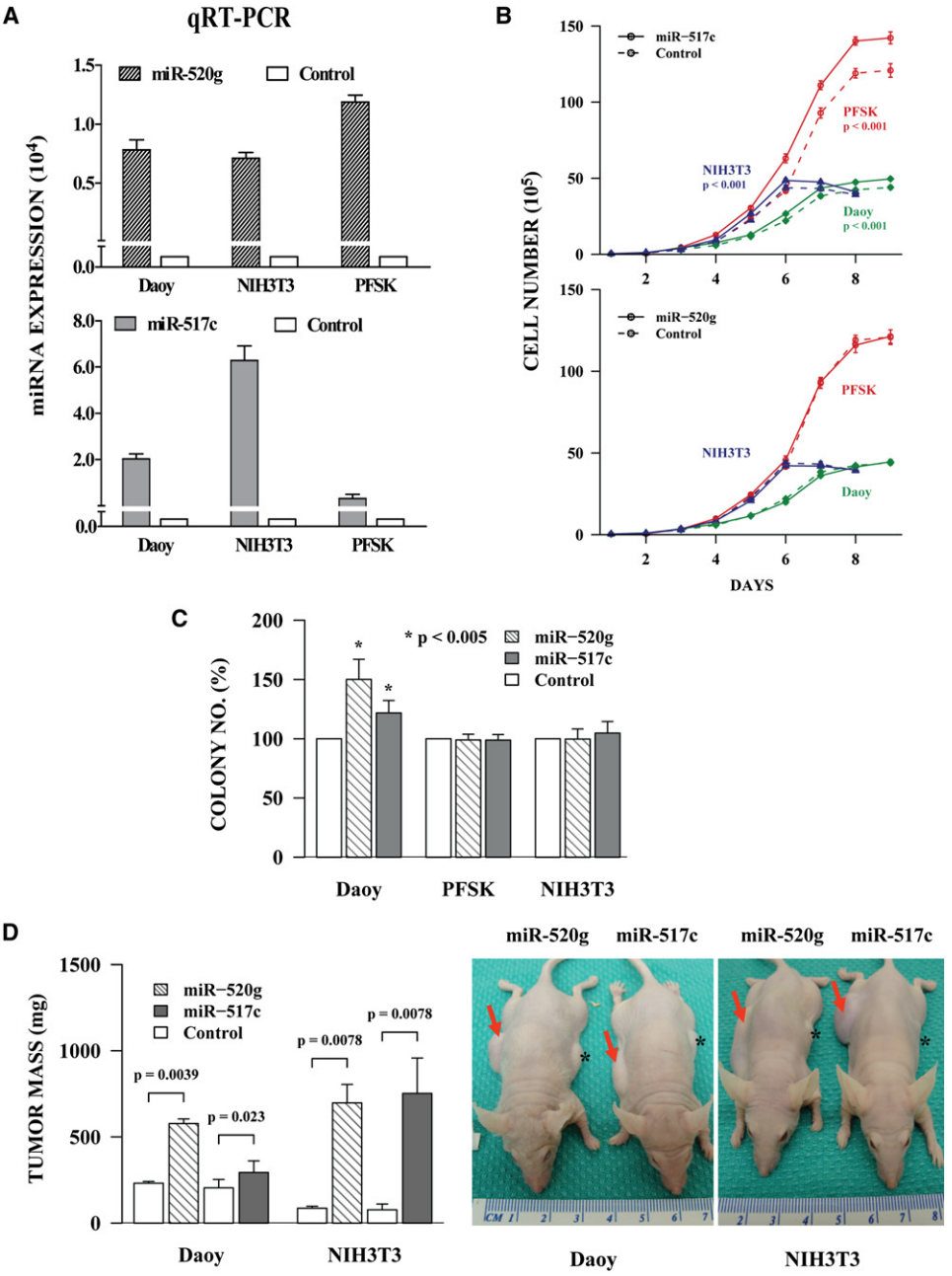

Figure 3. miR-520g and 517c Have Oncogenic Effects In Vitro and In Vivo

(A) Quantitative RT-PCR confirmation of stable miR-517c or 520g expression in PFSK, Daoy, and NIH 3T3 cell lines; miRNA levels are relative to RNU6B. Results are shown as means ± SD; n ≥ 2 to 3. Cell line pools were used for experiments shown in (B–D).

(B) Growth curves of miR-520g or 517c-expressing PFSK, Daoy, and NIH 3T3 stable cell lines indicate significant growth advantage in miR-517c (upper panel), but not miR-520g expressing (lower panel) cells in 10% serum conditions. Data represent three independent experiments with three replicas/data point; error bars, SD.

(C) MicroRNA 520g and 517c expression significantly enhances colony formation in Daoy, but not PFSK or NIH 3T3 cells; two independent soft agar growth assays with 3 replicas/data point are summarized, and error bars denote SD.

(D) Control and miR-520g or 517c expressing Daoy and NIH 3T3 stable cell lines were injected into contralateral flanks of *nu/nu* mice as described in methods. Histogram represents tumor weights from eight mice determined 6 weeks postinjection; error bars represent SEM. Right panel shows representative mice with Daoy or NIH 3T3 miR-520g or 517c associated xenografts (red arrow); *control injection sites.

CNS-PNET (Fogarty et al., 2005). Indeed, expression analysis revealed significant enrichment of developmental signaling genes, particularly those of the WNT pathway in *C19MC*-amplified CNS-PNET (Figure 4A; Table S6), indicating that one or more *C19MC* miRNA genes may function in WNT signaling. Notably, the WNT pathway, which plays a critical role in neural stem

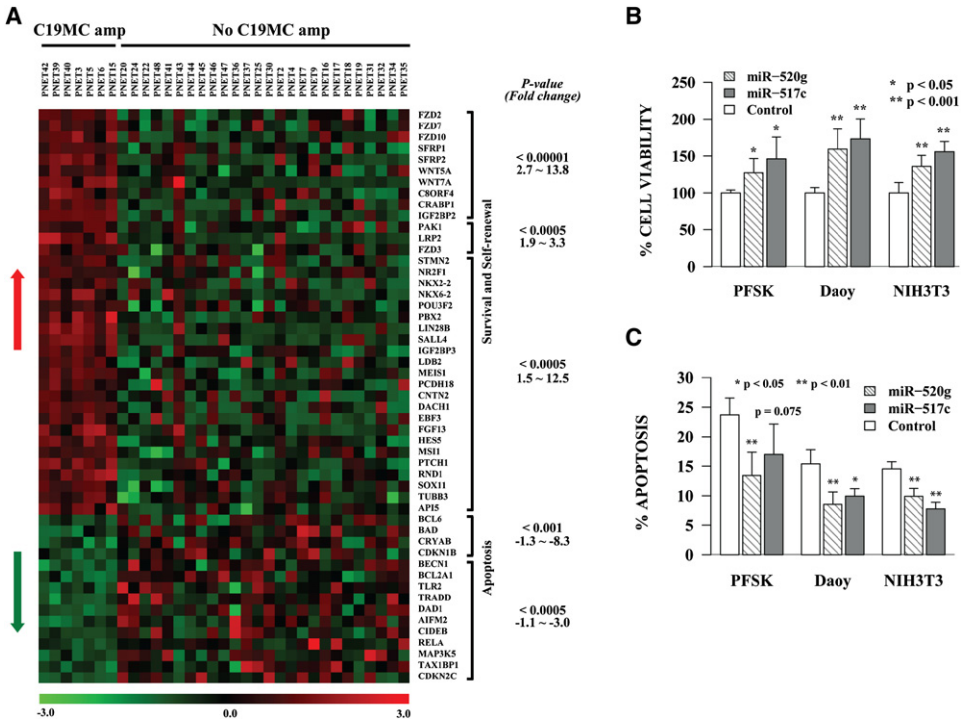

Figure 4. *C19MC* Amplification and Constitutive miR-517c and 520g Expression Is Associated with a Survival Phenotype

(A) Expression profiles demonstrate significant enrichment of self-renewal and survival genes in *C19MC*-amplified tumors. Heat map shows up (red arrow)- and down (green arrow)-regulated genes identified using a moderated t test statistic adjusted for multiple testing (FDR < 0.05) and analyzed for functional enrichment using GOSTAT (Tables S5 and S6). Significance and magnitude of gene expression changes between the two tumor groups are denoted respectively by p-value and fold change.

(B and C) PFSK, Daoy, and NIH 3T3 cells with stable miR-520g or 517c expression were exposed to 0.1% serum and assayed for cell viability or apoptosis relative to similarly treated control cells. (B) shows a representative plot of relative cell viability at 72 hr determined by trypan-blue staining; error bars represent SD; n = 3 with 3 replicas. (C) shows results of TUNEL assays in miR-520g and 517c stable and control lines at 72 hr after serum starvation; three experiments (two replicates/data point) are summarized; error bars represent SD, percent (%) apoptosis equal ratio of TUNEL to DAPI-positive cells.

cell survival and lineage determination (Kalani et al., 2008; Wexler et al., 2009), has been linked to miR-520g by recent computational studies (Gaidatzis et al., 2007). We focused on miR-520g to investigate signaling pathways associated with the *C19MC* oncogenic locus, as miR-520g expression correlated with the most robust phenotypic changes in hNSCs.

To uncover signaling pathways associated with miR-520g cellular phenotypes, we performed gene expression analysis of hNSC-miR-520g and PFSK-miR-520g and control cell line using the Illumina BeadChip arrays and used t tests to identify gene sets most significantly correlated with miR-520g expression. Not surprisingly, consistent with broad regulatory functions of miRNAs, we observed substantial gene expression changes in both hNSCs and PFSK cells with stable miR-520g expression; ~1000 to 5000 differentially expressed genes were respectively identified in PFSK and hNSC cell lines with miR-520g expression ($p < 0.05$). Functional analyses of miR-520g targets predicted by several different algorithms and of the miR-520g-associated gene sets determined from both cell line gene expression data consistently revealed most significant enrichment of genes with functions in neural development (data not shown). We therefore performed gene enrichment analysis on miR-520g-associated gene sets to investigate if developmental signaling pathways, which have been implicated in embryonal brain tumor development, including the WNT, SHH, NOTCH, and TGF-β pathways, were altered by miR-520g expression. We used the KEGG pathway database to identify and determine the number of specific pathway genes assayed by the Illumina BeadChip and applied multiple hypotheses testing to calculate relative representation of each pathway in the miR-520g-associated gene sets. Strikingly, consistent with observations in *C19MC*-amplified primary tumors ($p = 1.3E-5$), these analyses revealed most significant enrichment of WNT pathway loci in hNSC-miR-520g ($p = 1.3E-8$) and a similar more modest trend in PFSK-miR-520g cells ($p < 0.016$) (Table S7; Figure 6A).

The WNT pathway encodes a complex network of ligand and receptor combinations which signal via β-catenin-dependent (canonical) or independent (noncanonical) pathways in various cell contexts. While expression of WNT2/3 class ligands typically increase canonical WNT activity and upregulate downstream proliferative genes, such as *CCND1* and *MYCC*, the WNT5A ligand family classically activate noncanonical signaling but may also regulate the canonical pathway (Miller, 2002). Interestingly, in both hNSCs and PFSK cells, miR-520g expression correlated with upregulation of *WNT5A*, as well as *SFRP2/3* and *DKK1* genes, which encode antagonists of the canonical WNT pathway (Table S8). We confirmed upregulation of *WNT5A*, *SFRP2/3*, and *DKK1* in hNSCs and PFSK-miR-520g

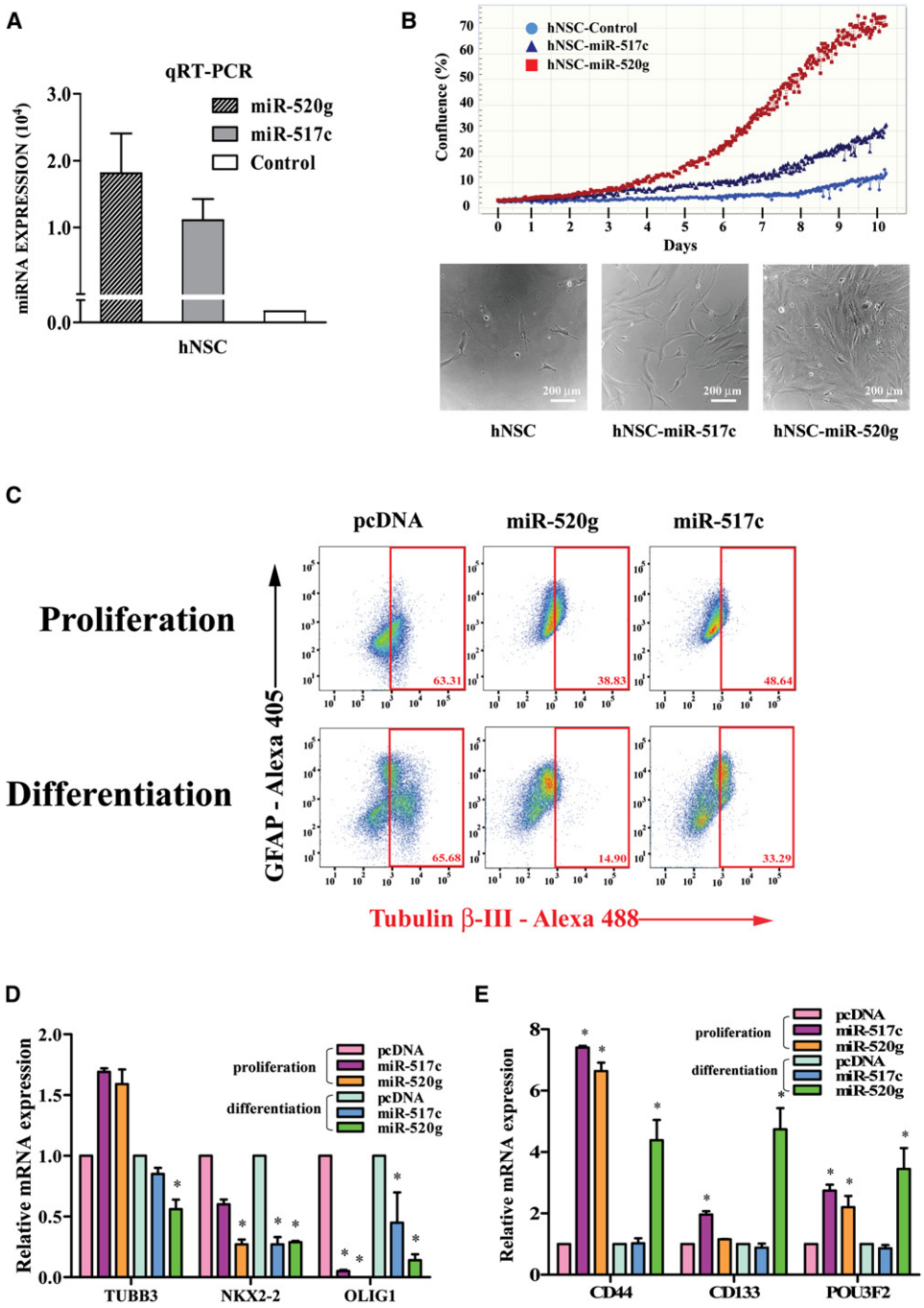

Figure 5. miR-520g and 517c Expression Drives Growth and Inhibits Differentiation of Human Neural Stem Cells

(A) Quantitative RT-PCR confirmation of stable miR-520g or 517c expression in hNSCs. Results are shown as means ± SD; n = 3; cell pools were used for all experiments.

(B) hNSCs-miR-520g and hNSCs-517c cell lines were exposed to differentiation media (DMEM +10% FBS) and monitored for changes in confluence with a live-cell imaging system. Photos on day 8 postdifferentiation (bottom panel) show no differences in cell mass; therefore, cell confluence was used to estimate cell numbers. In contrast to control cells, hNSC with stable miR-520g and 517c expression continued to grow in differentiation media.

(C) FACS analysis of stable hNSC-miR-520g and 517c and control pcDNA cell lines stained for neuronal (Tubulin βIII) and astrocytic (GFAP) lineage markers after growth in proliferative and differentiation media. GFAP expression was not consistently altered in miR-520g- and 517c-expressing cells (data not shown); Tubulin βIII expression (red boxes and D) was significantly diminished only in hNSCs-miR-520g cells grown in differentiation media.

(D and E) Quantitative RT-PCR analysis of cell lineage and stem cell markers in stable hNSC-miR-520g, 517c, and control hNSC-pcDNA cells grown under proliferative and differentiation conditions. Relative mRNA levels are normalized to 36B4 controls; *$p < 0.05$. Results shown are means ± SD; n = 2 to 3, with two replicas/experiment.

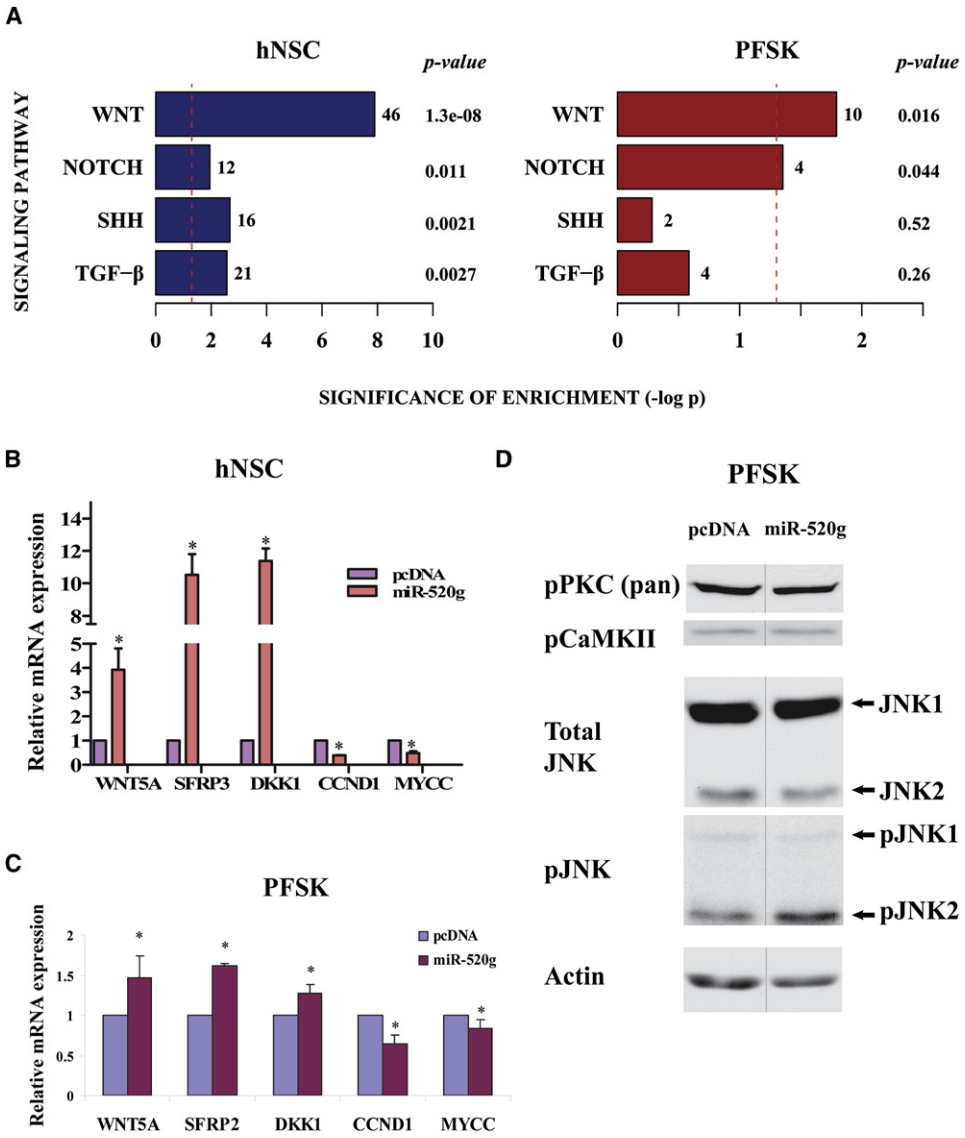

Figure 6. miR-520g Expression Correlates with Altered WNT Signaling

(A) Summary of pathway enrichment analysis performed on gene expression profiles of hNSCs (left panel) and PFSK (right panel) with stable miR-520g expression. Expression profiles of stable cell lines generated using Illumina BeadChips were compared to identify genes most significantly correlated with miR-520g expression in hNSC or PFSK cells. The miR-520g associated gene sets were then analyzed using the KEGG pathway database to determine significance of enrichment (–log10 [p value]) for specific developmental signaling pathways (bars) (Table S7). Number of genes in each pathway that meet the p value threshold (−log10 [$p < 0.05$], dashed line) is indicated.

(B and C) Quantitative RT-PCR analysis confirms WNT pathway dysregulation in miR-520g expressing stable hNSC and PFSK cell lines. In hNSCs (B) and PFSK (C) cells, miR-520g expression correlated with upregulation of WNT ligand, WNT5A, and WNT inhibitors—SFRP2/3 and DKK1. CCND1 and MYCC expression was diminished in miR-520g expressing cells but did not correlate with canonical WNT reporter activity (Figure S5). Results shown are means ± SD with n = 2, two replicas/experiment; mRNA levels are normalized to 36B4; *$p < 0.05$.

(D) Total lysates from control and stable PFSK-miR-520g cell lines were immunoblotted with phosphospecific antibodies for PKC (pPKC), CAMKII (pCAMKII), JNK1 and -2 (pJNK1, pJNK2), and antibodies for total JNK1 and -2; actin served as loading control. Arrows indicate higher levels of pJNK2, but not pJNK1, observed consistently in PFSK-miR-520g cells relative to controls without changes in total JNK1/2 levels; a representative of four independent experiments is shown.

cells by qRT-PCR analysis (Figures 6B and 6C). Of note, although expression of *CCND1* and *MYCC* was diminished in miR-520g expressing cells (Figure 6B and 6C), we did not observe significant changes in transcriptional activity of a TCF/LEF-driven reporter gene (pTOP-FLASH) in PFSK-miR-520g cells (Figure S5). These collective observations suggest that dysregulation of WNT pathway genes observed in miR-520g expressing stable cell lines and *C19MC*-amplified primary tumors may reflect altered noncanonical WNT signaling.

Downstream effectors and targets of noncanonical WNT signaling are poorly defined. It is known, however, that WNT5A can associate with specific Frizzled receptors to induce

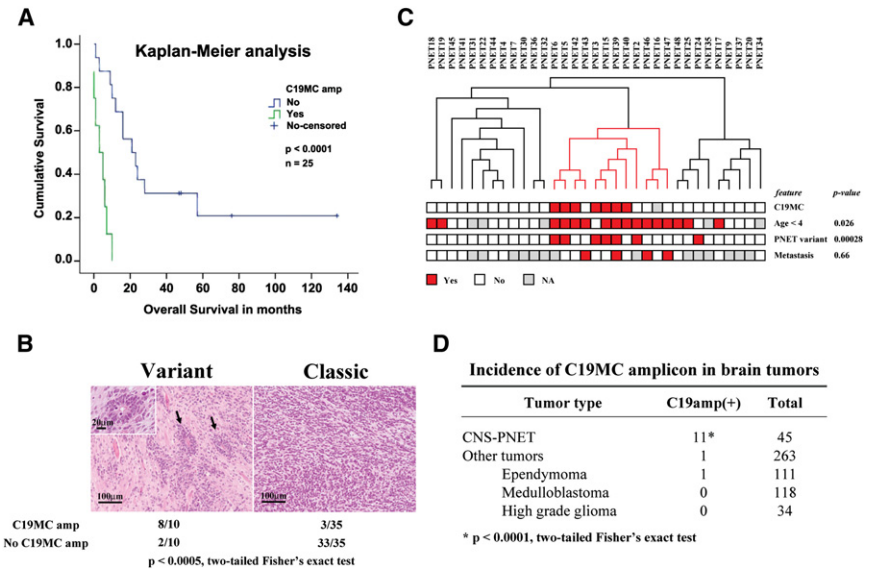

Figure 7. Amplification of the *C19MC* Locus Identifies CNS-PNET with Poor Survival and Distinct Tumor Pathology

(A) Kaplan-Meier survival estimates for patients stratified by *C19MC* amplification status in tumors; log-rank analysis correlate *C19MC* amplification with poorer overall survival.

(B) Representative micrograph illustrating variant and classic CNS-PNET histology and corresponding frequency of *C19MC* amplication. Variant histology distinguished by ependymal or ependymoblastic differentiation and distinct rosette structures (arrows) correlate significantly with *C19MC* amplication.

(C) Unsupervised hierarchical cluster analysis of expression profiles for 33 CNS-PNET is shown in relation to *C19MC* amplicon status and clinical characteristics of tumor (Table S1). Red and white boxes respectively denote presence or absence of clinical features, and gray boxes denote incomplete information. Cluster analyses show cosegregation (red cluster) and significant correlation of tumors with *C19MC* amplification or increased *C19MC* miRNA expression (Figure S7) with young age (<4 years) and variant histology, but not with tumor metastasis.

(D) Tabular summary indicating rarity of *C19MC* amplification in other pediatric brain tumors of different histologies. *C19MC* amplicon status was determined by FISH on tissue microarrays and/or SNP genotyping (CNS-PNET only).

noncanonical WNT signaling and activate several downstream effector kinases, including those of the Ca^{2+}-dependent PKC and CAMKII or the JNK pathways in various cell systems (Mikels and Nusse, 2006; Miller, 2002). To investigate if upregulation of WNT5A in CNS-PNET cells had any effect on noncanonical WNT signaling, we performed western blot analysis of PFSK-miR-520g cells using pan-PKC antibodies, which identify most Ca^{2+}-dependent phospho-PKC isoforms (PKC α, βI, βII), anti-phospho-CAMKII, as well total and phospho-specific JNK1/2 antibodies. Interestingly, whereas phospho-PKC or CAMKII levels were not altered with miR-520g expression, phospho-JNK2, but not JNK1 levels were consistently upregulated in PFSK cells with stable miR-520g expression as compared to controls (Figure 6D shows representative of four independent experiments), indicating that miR-520g maps upstream of JNK2. In aggregate, our data correlate increased expression of *WNT5A* and canonical WNT inhibitors, *SFRP2* and *DKK1*, with specific upregulation of phospho-JNK2 in PFSK-miR-520g cells, and indicate a role for miR-520g in noncanonical WNT/JNK2 signaling. These findings are particularly intriguing, as recent reports indicate canonical WNT activity may be linked to better survival in CNS-PNET (Rogers et al., 2009) and suggest *C19MC* amplification may portend poorer CNS-PNET phenotypes.

Amplification of the *C19MC* Locus Defines an Aggressive Group of CNS-PNET

To assess the significance of the *C19MC* locus in CNS-PNET pathogenesis, we investigated if *C19MC* amplification correlated with specific clinical features. Indeed, Kaplan Meier analysis of 25 evaluable patients revealed substantially poorer overall survival of patients with *C19MC*-amplified tumors (mean survival 4 ± 1.3 months in amplified versus 44 ± 12.8 months in nonamplified cases; $p < 0.0001$) (Figure 7A). Interestingly, the *C19MC* amplicon was also present at higher frequency in tumors with variant histological features of ependymal or ependymoblastic differentiation, (8/10 amplified versus 3/35 nonamplified tumors; $p < 0.0005$) and younger age at diagnosis (10/11 amplified versus 14/25 nonamplified CNS-PNETs were <4 yrs, $p < 0.026$) (Figures 7B and 7C). These collective data suggested that the *C19MC* amplicon may identify a CNS-PNET subgroup with distinct clinicopathological and genetic features. Consistent with this hypothesis, we observed cosegregation of *C19MC* amplified tumors in unsupervised cluster analysis of transcriptional profiles from 33 tumors (Figure 7C). Remarkably, in a survey of 263 other pediatric brain tumors by FISH analysis of tissue microarrays, we detected *C19MC* amplicon in only one non-CNS-PNET tumor (an ependymoma) ($p < 0.00001$) (Figure 7D). These data not only highlight the importance of the oncogenic *C19MC* locus in CNS-PNET pathogenesis but suggest that the *C19MC* locus may represent a specific marker for this tumor group.

DISCUSSION

In this study, we report the discovery of a large miRNA cluster on chr19q13.41, *C19MC*, that is frequently amplified in aggressive CNS-PNET and harbors miRNA oncogenes capable of driving growth of normal hNSCs. We provide evidence that miR-520g and 517c of the *C19MC* locus have oncogenic activity in vitro and in vivo, confers cell survival, and promotes primitive/progenitor cell phenotypes by attenuating differentiation of hNSCs. We correlate *C19MC* amplification in primary tumors and stable miR-520g expression in hNSC and CNS-PNET cells with robust dysregulation of WNT pathway loci and propose that *C19MC* miRNA oncogenes confer aggressive tumor phenotype in part by modulating WNT pathway signaling. Our findings have significant implications for clinical management of embryonal brain

tumors and provide exciting insights into the molecular pathogenesis of CNS-PNET and oncogenic properties of the *C19MC* locus.

Oncogenic Functions of the *C19MC* Locus

The functions of *C19MC* miRNAs are largely unknown; however, many exhibit restricted expression in undifferentiated/germinal tissues and cell types, such as placenta, testes (Bentwich et al., 2005), and hESCs (Bar et al., 2008; Laurent et al., 2008), indicating functions in cellular differentiation. Indeed, Bar et al. (2008) observed that expression of miR-520g, as well as four other *C19MC* miRNAs, diminishes with hESC differentiation. Intriguingly, they also demonstrate that *C19MC* may be regulated by *NANOG* and *OCT4*, known critical transcriptional regulators of ESC pluripotentcy, and propose that select *C19MC* miRNAs, including miR-520g, may mediate self-renewal and represent "signatures" of pluripotentcy in hESCs. In agreement with these studies, we observed that miR-520g and 517c increases growth of hNSCs under differentiation conditions. Importantly, our studies indicate that miR-520g and 517c expression not only confer increased cell survival but also promote stem/progenitor cell phenotypes. Therefore, we propose that aberrant expression of miR-520g and possibly other *C19MC* miRNAs alter normal neuroepithelial stem/precursor response to cell differentiation and survival stimuli and promote oncogenesis in part by enhancing target stem/progenitor cell pools available for additional transforming events. Notably, although both miR-520g and 517c cells confer cell survival in Daoy and PFSK tumor cells, we observed more limited effects of miR-520g and 517c on growth and differentiation phenotypes of these tumor cell lines (Figure S6), indicating that miR-520g and 517c may also manifest cell-stage and type restricted cellular effects/functions. Future in vivo experiments will be necessary to directly assess the individual and collective effects of miR-520g, 517c, as well other candidate *C19MC* miRNAs oncogenes, on survival and self-renewal properties of neural stem/progenitors cells.

A Role for miR-520g in WNT Signaling

We show that *C19MC* amplification and miR-520g expression strongly correlate with altered WNT signaling in primary tumors and stable tumor/hNSC cell lines, respectively. These findings, which concur with computational analyses of miR-520g (Gaidatzis et al., 2007), are particularly interesting as substantial evidence indicates aberrant WNT signaling may mediate malignant transformation by promoting stem/progenitor cell expansion in various developmental context, including the nervous system (Kalani et al., 2008; Reya and Clevers, 2005). Interestingly, WNT5A-mediated inhibition of canonical WNT signaling has been shown to enhance hematopoietic stem/progenitor cell repopulation (Nemeth et al., 2007). We observed decreased *CCND1* and *MYCC* expression in hNSCs and CNS-PNET cell line PFSK with stable miR-520g expression; however, reporter gene assays suggest that miR-520g does not significantly alter canonical WNT signaling in PFSK cells. Although the canonical WNT pathway has been most often highlighted in brain tumor development, our collective studies suggest that WNT5A-associated noncanonical WNT/JNK2 signaling, which is known to regulate cell polarity and neuronal maturation (Ciani and Salinas, 2005), is upregulated by miR-520g expression in hNSC and PFSK cells. The role of noncanonical WNT signaling in neural stem cells remains to be completely elucidated; however, our observations lead us to speculate that oncogenic miR-520g, and possibly other related *C19MC* miRNA, promotes transformation of neural stem/progenitor cell pools by subverting WNT signaling.

While our aggregate data links miR-520g with altered WNT signaling, the mechanism(s) by which miR-520g mediates this effect remains to be determined. An analysis of miR-520 g-associated gene sets in PFSK and hNSCs revealed few genes that represented strong direct miR-520g targets, based on criteria of target site prediction by at least 2 of 3 target prediction programs and modest to strong conservation of target sites (Watanabe et al., 2007). However, a comparative analysis of 2460 miR-520g target genes predicted by three algorithms (Table S9) reveal a common set of 63 candidate genes, a subset of which (*TLE4*, *PRICKLE 2*, *BMP6*, *CAMK2N1*, *CUL3*, *LHX8*, and *MAPRE1/EB1*), represent promising candidates, as they are implicated in WNT signaling and also exhibit one or more conserved miR-520g binding sites. Our studies to date reveal only limited gene expression changes of most candidate targets in miR-520g expressing stable hNSC and PFSK cell lines; therefore, high-throughput reporter gene assays and proteomic analysis are underway to validate these predicted miR-520g targets.

It is important to point out that the three algorithms used for identification of candidate miR-520g targets in our study rely largely on sequence conservation. Although use of evolutionary conservation has represented a key methodological advance for target gene identification of highly conserved miRNAs, the importance of such parameters for defining targets of poorly conserved, primate-specific miRNAs, such as those of the *C19MC* locus, remain unknown (Bartel, 2009). Significantly, functionally validated targets without matched seed pairing have been reported for a number of miRNAs including LIN28 (Wu and Belasco, 2005) and miR-24 (Lal et al., 2009). Targeting of "seedless" 3′UTR may represent a particularly important mechanism for *C19MC* miRNAs, as they are characterized by poorly defined seed sequence; thus, conventional seed-matched algorithms as used in this study may only identify a small subset of biologically relevant miR-520g targets.

Notably, many predicted miR-520g target genes also contain binding sites for other candidate *C19MC* miRNA oncogenes, including miR-517c and miR-519a. As recent studies indicate that most miRNAs individually only have modest, modulatory effects on gene transcription or translation (Baek et al., 2008; Selbach et al., 2008), it is likely that miR-520g will require cooperativity with other noncoding or coding loci to effect robust changes in gene regulation and cell signaling. In this regard, it is interesting to note that in our study, we observed frequent gains of chr2 in tumors with *C19MC* amplification; thus, in addition to other *C19MC* miRNAs, which are overexpressed in CNS-PNET, we speculate that one or more loci on chr2 may also encode oncogenic partners of miR-520g.

Clinical Implications

Current treatment of malignant pediatric brain tumors with chemo-radiotherapy engenders significant long-term neurocognitive sequelae; therefore, there is substantial interest in applying

molecular markers to optimize treatment. In addition to potential applications in tumor diagnosis, our data suggest the *C19MC* locus may also have a prognostic role. A recent report described the *C19MC* amplicon in a case of an embryonal brain tumor characterized by ependymoblastic differentiation and proposed association of *C19MC* with a specific nosologic entity (Pfister et al., 2009). However, our studies indicate a significant, but not exclusive, correlation of *C19MC* amplification with histology, pointing to a broader role for the *C19MC* locus in CNS-PNET pathogenesis. Specifically, a proportion of tumors that segregate with the *C19MC*-amplified tumors lack characteristic histology or *C19MC* amplification but exhibit increased expression of select *C19MC* miRNA oncogenes (Figure S7) and/or chr2 gains. Future investigations of alternative mechanisms of *C19MC* activation and/or other cooperating oncogenic loci suggested by our studies will be an important step toward delineating the scope of *C19MC* functions and how they contribute to the molecular pathogenesis of CNS-PNET.

Although the effects of treatment-related parameters could not be fully evaluated in our patient cohort, the collective data from this study provides a compelling basis for investigating the *C19MC* locus as a biomarker in larger, homogenously treated cohorts of CNS-PNET. As our experimental data link WNT pathway dysregulation with oncogenic functions of the *C19MC* miRNAs, it will also be of interest to determine whether tumor phenotypes correlate with specific patterns of WNT pathway activity.

We have identified recurrent amplification leading to overexpression of the *C19MC* locus in a human cancer and demonstrate that at least 2 members of the cluster mediate oncogenic effects. Our data links the *C19MC* amplicon to a distinctly aggressive clinical phenotype and point to promising diagnostic and therapeutic applications of this locus for pediatric embryonal brain tumors. Together with recent reports that implicate *C19MC* miRNAs in aggressive primary breast cancer (Foekens et al., 2008), our findings suggest activation of the *C19MC* locus may generally define aggressive human tumors. Combined with recent success in blood-based detection (Mitchell et al., 2008) and in vivo targeting of oncogenic miRNAs (Krutzfeldt et al., 2005), our findings raise exciting possibilities to exploit *C19MC* as a diagnostic tool and therapeutic target for a broader spectrum of human cancers.

EXPERIMENTAL PROCEDURES

Tumor and Nucleic Acid Samples

Tumor samples and clinical information were collected with consent as per protocols approved by the Hospital Research Ethics Board at participating institutions (listed in Supplemental Data). Clinicopathological data is listed in Table S1. Only tumors classified as CNS-PNET according to 2007 WHO CNS tumor classification criteria (McLendon et al., 2007) were included. DNA and RNA were extracted by standard methods; tumor histology was reviewed by CH or CE. Pediatric brain tumor tissue microarrays were previously described (Liang et al., 2008; Ray et al., 2004; Tabori et al., 2006).

Microarray and Fluorescence In Situ Hybridization Analysis

DNA and RNA array hybridizations were carried out by The Centre of Applied Genomics Facility (TCAG), Hospital for Sick Children, Toronto (http://www.tcag.ca/), using the Affymetrix 500K/250K NspI and 250 StyI GeneChip Mapping arrays and the Illumina Human-6 V2 BeadChip array (http://www.illumina.com), respectively. Hybridization methods, data collection, and analysis are detailed in Supplemental Data. Dual-colored fluorescence in situ hybridization (FISH) analyses were performed using prelabeled BAC probes as detailed in Supplemental Data.

Immunoblot Assays and Quantitative Real-Time PCR Analysis for DNA and mRNA

See Supplemental Data available online.

MicroRNA Expression Analysis with TaqMan MicroRNA Arrays and qRT-PCR

See Supplemental Data available online.

Stable microRNA expression

To generate miR 517c and 520g expression plasmids, synthetic oligonucleotides (Integrated DNA Technologies) containing mature miR-517c or miR-520g and 25–40 bp of flanking precursor miRNAs sequences (Accession MI0003166 and M10003174, respectively, from http://microrna.sanger.ac.uk/sequences) were cloned into a pcDNA3 vector (Invitrogen). Plasmid sequences are available upon request. Stable cell lines were generated by transfecting Daoy, NIH 3T3, and PFSK cells with pcDNA-miR-520g, miR-517c, or empty vector cells selected in G418 (2.5 μg/ml) were tested for miRNA expression by qRT-PCR.

Cell Line Propagation, Growth, Survival, and Transformation Assays

See Supplemental Data available online.

Nude Mice Xenograft Assays

Protocols for animal experimentation were approved by the Hospital for Sick Children Animal Care Committee and are described in Supplemental Data.

Human Neural Stem Cell Line Propagation, Growth, and Differentiation Assays

An adherent human neural stem (hNSC) cell line was generated from a 50-day-old fetal cortex with consent obtained under a Hospital for Sick Children Research Ethics Board approved protocol and characterized according to published methods (Sun et al., 2008). The hNSC line was propagated in RHB-A media (Stem Cell Sciences Ltd.) with recombinant murine EGF and human FGF-2 (10 ng/ml final concentration; Peprotech). Stable hNSC lines were generated by nucleofection (Amaxa Biosystems) with pcDNA-miR-520g and 517c plasmids and selection in G418-containing media for 14 days. For growth assays, stable hNSCs-miR-520g and 517c cell lines were plated in 96-well dishes at 1000 cells/well, allowed to attach overnight under proliferative conditions, and then switched to DMEM +10% FBS and monitored for growth using an InCyte imaging system (Essen Instruments) or MTT assay as described in Supplemental Data. Expression of differentiation markers in stable miR-520 and 517c expressing hNSCs was determined using FACS analysis with anti-Tubulin β-III (TuJ1 antibodies, 1:500, Chemicon), anti-GFAP (1:300, monoclonal GA-5, Sigma monoclonal), and Alexa 405 or 488 anti-species antibodies (Invitrogen) as described previously (Pollard et al., 2009).

Statistical Analyses

ANOVA method was used for time-series cell growth and survival experiments. Significance of soft agar assays and correlation of gene expression with chr19q13.41 amplification was determined using unpaired, two-tailed Student's t tests; p values were adjusted for multiple testing by FDR method for comparison of tumor or cell line gene-expression profiles. A Wilcoxon rank sum test was used to determine significance of xenograft studies. Correlation of amplicon to survival was assessed using the Kaplan Meier method and log-rank test ($\alpha = 0.05$) and to age and histology by a two-sided Fisher's exact test.

ACCESSION NUMBERS

Microarray data from this study are available at NCBI Gene Expression Omnibus (http://www.ncbi.nlm.nih.gov/geo/) under accession numbers GSE14296 and GSE16988.

SUPPLEMENTAL DATA

Supplemental Data include seven figures and nine tables and can be found with this article online at http://www.cell.com/cancer-cell/supplemental/S1535-6108(09)00388-2.

ACKNOWLEDGMENTS

We thank P. Burger, J. Squire, and L. Penn for mentorship; M. Massimo, L. Lafay-Cousin, M. Zielenska, S. Chilton, P. Northcott, P. Kongkam, T. Paton, and G. Casallo for generous help; J. Dick, S. Egan, C.C. Hui, E. Lechman, R. Gilbertson, and W. Halliday for helpful discussions; and P. Hu for statistical analysis. Funding from CBTF, SickKids (Brainchild), JM Foundations, and CCSRI (grant no. 17473) to A.H.; AIRC to P.M.; and tissue contributions from CHTN, NINDs, and the London Regional Brain Tumor Bank are gratefully acknowledged. M.L. was an ABTA Fellow; K.F.L. and D.S. received SickKids foundation RESTRACOMP predoctoral awards. M.L., K.F.L., Y.L., and D.S. performed all experiments and analyses with support from D.P., L.Z., and P.B. NSC studies were performed by I.C; E.B., P.M., M.L., P.C., M.C., T.V., S.P., C.E., and C.L. provided tumor tissue and clinical data. A.H. supervised the project. A.H., M.D.T., S.S., J.T.R., C.E.H., and P.B.D. contributed to manuscript writing and review.

Received: February 2, 2009
Revised: August 3, 2009
Accepted: October 23, 2009
Published: December 7, 2009

REFERENCES

Allen, J.C., Judkins, A.R., Rosenblum, M.K., and Biegel, J.A. (2006). Atypical teratoid/rhabdoid tumor evolving from an optic pathway ganglioglioma: case study. Neuro-oncol. *8*, 79–82.

Baek, D., Villen, J., Shin, C., Camargo, F.D., Gygi, S.P., and Bartel, D.P. (2008). The impact of microRNAs on protein output. Nature *455*, 64–71.

Bar, M., Wyman, S.K., Fritz, B.R., Qi, J., Garg, K.S., Parkin, R.K., Kroh, E.M., Bendoraite, A., Mitchell, P.S., Nelson, A.M., et al. (2008). MicroRNA discovery and profiling in human embryonic stem cells by deep sequencing of small RNA libraries. Stem Cells *26*, 2496–2505.

Bartel, D.P. (2009). MicroRNAs: target recognition and regulatory functions. Cell *136*, 215–233.

Beissbarth, T., and Speed, T.P. (2004). GOstat: find statistically overrepresented Gene Ontologies within a group of genes. Bioinformatics *20*, 1464–1465.

Bentwich, I., Avniel, A., Karov, Y., Aharonov, R., Gilad, S., Barad, O., Barzilai, A., Einat, P., Einav, U., Meiri, E., et al. (2005). Identification of hundreds of conserved and nonconserved human microRNAs. Nat. Genet. *37*, 766–770.

Bonci, D., Coppola, V., Musumeci, M., Addario, A., Giuffrida, R., Memeo, L., D'Urso, L., Pagliuca, A., Biffoni, M., Labbaye, C., et al. (2008). The miR-15a-miR-16–1 cluster controls prostate cancer by targeting multiple oncogenic activities. Nat. Med. *14*, 1271–1277.

Briscoe, J., Pierani, A., Jessell, T.M., and Ericson, J. (2000). A homeodomain protein code specifies progenitor cell identity and neuronal fate in the ventral neural tube. Cell *101*, 435–445.

Burger, P.C. (2006). Supratentorial primitive neuroectodermal tumor (sPNET). Brain Pathol. *16*, 86.

Calin, G.A., Dumitru, C.D., Shimizu, M., Bichi, R., Zupo, S., Noch, E., Aldler, H., Rattan, S., Keating, M., Rai, K., et al. (2002). Frequent deletions and down-regulation of micro- RNA genes miR15 and miR16 at 13q14 in chronic lymphocytic leukemia. Proc. Natl. Acad. Sci. USA *99*, 15524–15529.

Ciani, L., and Salinas, P.C. (2005). WNTs in the vertebrate nervous system: from patterning to neuronal connectivity. Nat. Rev. Neurosci. *6*, 351–362.

Esquela-Kerscher, A., and Slack, F.J. (2006). Oncomirs - microRNAs with a role in cancer. Nat. Rev. Cancer *6*, 259–269.

Fangusaro, J., Finlay, J., Sposto, R., Ji, L., Saly, M., Zacharoulis, S., Asgharzadeh, S., Abromowitch, M., Olshefski, R., Halpern, S., et al. (2008). Intensive chemotherapy followed by consolidative myeloablative chemotherapy with autologous hematopoietic cell rescue (AuHCR) in young children with newly diagnosed supratentorial primitive neuroectodermal tumors (sPNETs): report of the Head Start I and II experience. Pediatr. Blood Cancer *50*, 312–318.

Foekens, J.A., Sieuwerts, A.M., Smid, M., Look, M.P., de Weerd, V., Boersma, A.W., Klijn, J.G., Wiemer, E.A., and Martens, J.W. (2008). Four miRNAs associated with aggressiveness of lymph node-negative, estrogen receptor-positive human breast cancer. Proc. Natl. Acad. Sci. USA *105*, 13021–13026.

Fogarty, M.P., Kessler, J.D., and Wechsler-Reya, R.J. (2005). Morphing into cancer: the role of developmental signaling pathways in brain tumor formation. J. Neurobiol. *64*, 458–475.

Gaidatzis, D., van Nimwegen, E., Hausser, J., and Zavolan, M. (2007). Inference of miRNA targets using evolutionary conservation and pathway analysis. BMC Bioinformatics *8*, 69.

Gessi, M., Giangaspero, F., Lauriola, L., Gardiman, M., Scheithauer, B.W., Halliday, W., Hawkins, C., Rosenblum, M.K., Burger, P.C., and Eberhart, C.G. (2009). Embryonal Tumors With Abundant Neuropil and True Rosettes: A Distinctive CNS Primitive Neuroectodermal Tumor. Am. J. Surg. Pathol. *33*, 211–217.

He, L., Thomson, J.M., Hemann, M.T., Hernando-Monge, E., Mu, D., Goodson, S., Powers, S., Cordon-Cardo, C., Lowe, S.W., Hannon, G.J., and Hammond, S.M. (2005). A microRNA polycistron as a potential human oncogene. Nature *435*, 828–833.

Iafrate, A.J., Feuk, L., Rivera, M.N., Listewnik, M.L., Donahoe, P.K., Qi, Y., Scherer, S.W., and Lee, C. (2004). Detection of large-scale variation in the human genome. Nat. Genet. *36*, 949–951.

Inda, M.M., Perot, C., Guillaud-Bataille, M., Danglot, G., Rey, J.A., Bello, M.J., Fan, X., Eberhart, C., Zazpe, I., Portillo, E., et al. (2005). Genetic heterogeneity in supratentorial and infratentorial primitive neuroectodermal tumours of the central nervous system. Histopathology *47*, 631–637.

Johnson, S.M., Grosshans, H., Shingara, J., Byrom, M., Jarvis, R., Cheng, A., Labourier, E., Reinert, K.L., Brown, D., and Slack, F.J. (2005). RAS is regulated by the let-7 microRNA family. Cell *120*, 635–647.

Judkins, A.R., and Ellison, D.W. (2008). Ependymoblastoma: Dear, Damned, Distracting Diagnosis, Farewell!. Brain Pathol. Published online December 17, 2008. 10.1111/j.1750-3639.2008.00253.x.

Kalani, M.Y., Cheshier, S.H., Cord, B.J., Bababeygy, S.R., Vogel, H., Weissman, I.L., Palmer, T.D., and Nusse, R. (2008). Wnt-mediated self-renewal of neural stem/progenitor cells. Proc. Natl. Acad. Sci. USA *105*, 16970–16975.

Krutzfeldt, J., Rajewsky, N., Braich, R., Rajeev, K.G., Tuschl, T., Manoharan, M., and Stoffel, M. (2005). Silencing of microRNAs in vivo with 'antagomirs'. Nature *438*, 685–689.

Lal, A., Navarro, F., Maher, C.A., Maliszewski, L.E., Yan, N., O'Day, E., Chowdhury, D., Dykxhoorn, D.M., Tsai, P., Hofmann, O., et al. (2009). miR-24 Inhibits cell proliferation by targeting E2F2, MYC, and other cell-cycle genes via binding to "seedless" 3′UTR microRNA recognition elements. Mol. Cell *35*, 610–625.

Laurent, L.C., Chen, J., Ulitsky, I., Mueller, F.J., Lu, C., Shamir, R., Fan, J.B., and Loring, J.F. (2008). Comprehensive microRNA profiling reveals a unique human embryonic stem cell signature dominated by a single seed sequence. Stem Cells *26*, 1506–1516.

Liang, M.L., Ma, J., Ho, M., Solomon, L., Bouffet, E., Rutka, J.T., and Hawkins, C. (2008). Tyrosine kinase expression in pediatric high grade astrocytoma. J. Neurooncol. *87*, 247–253.

Lin, M., Wei, L.J., Sellers, W.R., Lieberfarb, M., Wong, W.H., and Li, C. (2004). dChipSNP: significance curve and clustering of SNP-array-based loss-of-heterozygosity data. Bioinformatics *20*, 1233–1240.

Lu, J., Getz, G., Miska, E.A., Alvarez-Saavedra, E., Lamb, J., Peck, D., Sweet-Cordero, A., Ebert, B.L., Mak, R.H., Ferrando, A.A., et al. (2005). MicroRNA expression profiles classify human cancers. Nature *435*, 834–838.

McCabe, M.G., Ichimura, K., Liu, L., Plant, K., Backlund, L.M., Pearson, D.M., and Collins, V.P. (2006). High-resolution array-based comparative genomic hybridization of medulloblastomas and supratentorial primitive neuroectodermal tumors. J. Neuropathol. Exp. Neurol. *65*, 549–561.

McLendon, R.E., Judkins, A.R., Eberhart, C.G., Fuller, G.N., Sarkar, C., and Ng., H.-K., (2007). Central nervous system Primitive Neuroectodermal Tumors (PNET). In WHO Classification of Tumors of the Central Nervous System, B.W. Scheithauer, G.N. Fuller, and S.R. VandenBerg, eds. (Lyon: IARC Press), pp. 141–146.

Mikels, A.J., and Nusse, R. (2006). Purified Wnt5a protein activates or inhibits beta-catenin-TCF signaling depending on receptor context. PLoS Biol. *4*, e115. 10.1371/journal.pbio.0040115.

Miller, J.R. (2002). The Wnts. Genome Biol. *3*, REVIEWS3001.

Mitchell, P.S., Parkin, R.K., Kroh, E.M., Fritz, B.R., Wyman, S.K., Pogosova-Agadjanyan, E.L., Peterson, A., Noteboom, J., O'Briant, K.C., Allen, A., et al. (2008). Circulating microRNAs as stable blood-based markers for cancer detection. Proc. Natl. Acad. Sci. USA *105*, 10513–10518.

Nemeth, M.J., Topol, L., Anderson, S.M., Yang, Y., and Bodine, D.M. (2007). Wnt5a inhibits canonical Wnt signaling in hematopoietic stem cells and enhances repopulation. Proc. Natl. Acad. Sci. USA *104*, 15436–15441.

Packer, R.J., Gajjar, A., Vezina, G., Rorke-Adams, L., Burger, P.C., Robertson, P.L., Bayer, L., LaFond, D., Donahue, B.R., Marymont, M.H., et al. (2006). Phase III study of craniospinal radiation therapy followed by adjuvant chemotherapy for newly diagnosed average-risk medulloblastoma. J. Clin. Oncol. *24*, 4202–4208.

Papagiannakopoulos, T., Shapiro, A., and Kosik, K.S. (2008). MicroRNA-21 targets a network of key tumor-suppressive pathways in glioblastoma cells. Cancer Res. *68*, 8164–8172.

Pfister, S., Remke, M., Castoldi, M., Bai, A.H., Muckenthaler, M.U., Kulozik, A., von Deimling, A., Pscherer, A., Lichter, P., and Korshunov, A. (2009). Novel genomic amplification targeting the microRNA cluster at 19q13.42 in a pediatric embryonal tumor with abundant neuropil and true rosettes. Acta Neuropathol. *117*, 457–464. Published online December 5, 2008. 10.1007/s00401-008-0467-y.

Pfister, S., Remke, M., Toedt, G., Werft, W., Benner, A., Mendrzyk, F., Wittmann, A., Devens, F., von Hoff, K., Rutkowski, S., et al. (2007). Supratentorial primitive neuroectodermal tumors of the central nervous system frequently harbor deletions of the CDKN2A locus and other genomic aberrations distinct from medulloblastomas. Genes Chromosomes Cancer *46*, 839–851.

Pollard, S.M., Yoshikawa, K., Clarke, I.D., Danovi, D., Stricker, S., Russell, R., Bayani, J., Head, R., Lee, M., Bernstein, M., et al. (2009). Glioma stem cell lines expanded in adherent culture have tumor-specific phenotypes and are suitable for chemical and genetic screens. Cell Stem Cell *4*, 568–580.

Pomeroy, S.L., Tamayo, P., Gaasenbeek, M., Sturla, L.M., Angelo, M., McLaughlin, M.E., Kim, J.Y., Goumnerova, L.C., Black, P.M., Lau, C., et al. (2002). Prediction of central nervous system embryonal tumour outcome based on gene expression. Nature *415*, 436–442.

Ray, A., Ho, M., Ma, J., Parkes, R.K., Mainprize, T.G., Ueda, S., McLaughlin, J., Bouffet, E., Rutka, J.T., and Hawkins, C.E. (2004). A clinicobiological model predicting survival in medulloblastoma. Clin. Cancer Res. *10*, 7613–7620.

Reya, T., and Clevers, H. (2005). Wnt signalling in stem cells and cancer. Nature *434*, 843–850.

Rogers, H.A., Miller, S., Lowe, J., Brundler, M.A., Coyle, B., and Grundy, R.G. (2009). An investigation of WNT pathway activation and association with survival in central nervous system primitive neuroectodermal tumours (CNS PNET). Br. J. Cancer *100*, 1292–1302.

Selbach, M., Schwanhausser, B., Thierfelder, N., Fang, Z., Khanin, R., and Rajewsky, N. (2008). Widespread changes in protein synthesis induced by microRNAs. Nature *455*, 58–63.

Sun, Y., Pollard, S., Conti, L., Toselli, M., Biella, G., Parkin, G., Willatt, L., Falk, A., Cattaneo, E., and Smith, A. (2008). Long-term tripotent differentiation capacity of human neural stem (NS) cells in adherent culture. Mol. Cell. Neurosci. *38*, 245–258.

Tabori, U., Ma, J., Carter, M., Zielenska, M., Rutka, J., Bouffet, E., Bartels, U., Malkin, D., and Hawkins, C. (2006). Human telomere reverse transcriptase expression predicts progression and survival in pediatric intracranial ependymoma. J. Clin. Oncol. *24*, 1522–1528.

Timmermann, B., Kortmann, R.D., Kuhl, J., Rutkowski, S., Meisner, C., Pietsch, T., Deinlein, F., Urban, C., Warmuth-Metz, M., and Bamberg, M. (2006). Role of radiotherapy in supratentorial primitive neuroectodermal tumor in young children: results of the German HIT-SKK87 and HIT-SKK92 trials. J. Clin. Oncol. *24*, 1554–1560.

Voorhoeve, P.M., le Sage, C., Schrier, M., Gillis, A.J., Stoop, H., Nagel, R., Liu, Y.P., van Duijse, J., Drost, J., Griekspoor, A., et al. (2006). A genetic screen implicates miRNA-372 and miRNA-373 as oncogenes in testicular germ cell tumors. Cell *124*, 1169–1181.

Watanabe, Y., Tomita, M., and Kanai, A. (2007). Computational methods for microRNA target prediction. Methods Enzymol. *427*, 65–86.

Wexler, E.M., Paucer, A., Kornblum, H.I., Plamer, T.D., and Geschwind, D.H. (2009). Endogenous Wnt signaling maintains neural progenitor cell potency. Stem Cells *27*, 1130–1141.

Wu, L., and Belasco, J.G. (2005). Micro-RNA regulation of the mammalian lin-28 gene during neuronal differentiation of embryonal carcinoma cells. Mol. Cell. Biol. *25*, 9198–9208.

Zhou, Q., and Anderson, D.J. (2002). The bHLH transcription factors OLIG2 and OLIG1 couple neuronal and glial subtype specification. Cell *109*, 61–73.

Zindy, F., Nilsson, L.M., Nguyen, L., Meunier, C., Smeyne, R.J., Rehg, J.E., Eberhart, C., Sherr, C.J., and Roussel, M.F. (2003). Hemangiosarcomas, medulloblastomas, and other tumors in Ink4c/p53-null mice. Cancer Res. *63*, 5420–5427.